

Journal Pre-proof

Environmental Life Cycle Assessment of Encapsulated Rejuvenators from Mining Truck Waste Tires via Pyrolysis for Asphalt Self-Healing

Luis E. Arteaga-Pérez, Sebastián Larrere, Manuel Chávez-Delgado, Yesid J. Rueda Ordoñez, Jose L. Concha, Cristina Segura, Jose Norambuena-Contreras, Yannay Casas-Ledón

PII: S0959-6526(25)00137-4

DOI: <https://doi.org/10.1016/j.jclepro.2025.144787>

Reference: JCLP 144787

To appear in: *Journal of Cleaner Production*

Received Date: 8 August 2024

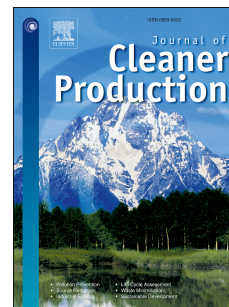
Revised Date: 29 December 2024

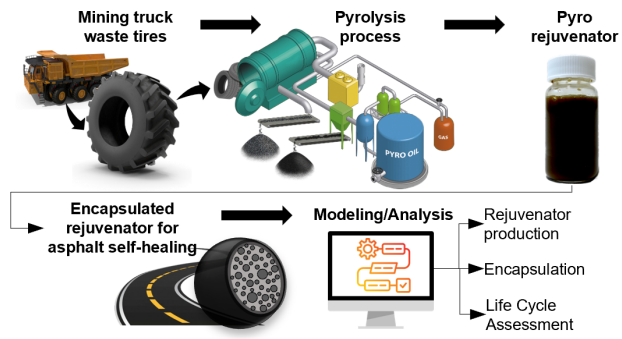
Accepted Date: 14 January 2025

Please cite this article as: Arteaga-Pérez LE, Larrere S, Chávez-Delgado M, Rueda Ordoñez YJ, Concha JL, Segura C, Norambuena-Contreras J, Casas-Ledón Y, Environmental Life Cycle Assessment of Encapsulated Rejuvenators from Mining Truck Waste Tires via Pyrolysis for Asphalt Self-Healing, *Journal of Cleaner Production*, <https://doi.org/10.1016/j.jclepro.2025.144787>.

This is a PDF file of an article that has undergone enhancements after acceptance, such as the addition of a cover page and metadata, and formatting for readability, but it is not yet the definitive version of record. This version will undergo additional copyediting, typesetting and review before it is published in its final form, but we are providing this version to give early visibility of the article. Please note that, during the production process, errors may be discovered which could affect the content, and all legal disclaimers that apply to the journal pertain.

© 2025 Published by Elsevier Ltd.





Journal Pre-proof

Environmental Life Cycle Assessment of Encapsulated Rejuvenators from Mining Truck Waste Tires via Pyrolysis for Asphalt Self-Healing

Luis E. Arteaga-Pérez¹, Sebastián Larrere^{1,2}, Manuel Chávez-Delgado^{3,4}, Yesid J. Rueda Ordoñez⁵, Jose L. Concha³, Cristina Segura⁶, Jose Norambuena-Contreras⁷, Yannay Casas-Ledón^{2*}

¹ Department of Chemical Engineering, Faculty of Engineering, Universidad de Concepcion, Concepción, 4030000, Chile.

² Department of Environmental Engineering, Environmental Sciences Faculty and Center EULA-Chile, Universidad de Concepción, Concepción, 4030000, Chile.

³ LabMAT, Department of Civil and Environmental Engineering, Faculty of Engineering, Universidad del Bío-Bío, Concepción, 4051381, Chile.

⁴ Departamento de Ingeniería Civil, Facultad de Ingeniería, Sede Concepción, Universidad Andres Bello, Chile.

⁵ Research Group on Energy and Environment (GIEMA), School of Mechanical Engineering, Universidad Industrial de Santander, Carrera 27 Calle 9, Bucaramanga 680002, Colombia.

⁶ Technological Development Unit-UDT, Universidad de Concepcion, Cordillera, 2634, Coronel, 4191996, Chile.

⁷ Materials and Manufacturing Research Institute, Department of Civil Engineering, Faculty of Science and Engineering, Swansea University, SA1 8EN, UK.

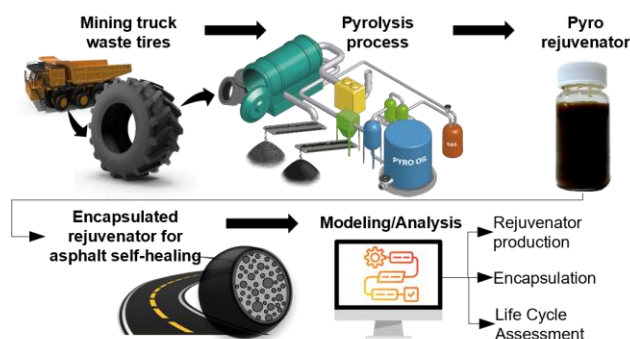
*Corresponding author: ycasas@udec.cl

Abstract

The application of pyrolysis to convert waste tires into fuels and engineering additives for asphalt self-healing is being actively explored by both industry stakeholders and researchers. This study presents, for the first time, a comprehensive evaluation of the technical and environmental implications of producing encapsulated liquid pyro-rejuvenators for asphalt self-healing applications. The analyses include experimental data on the production, characterization, and upgrading of crude pyro-oils, complemented by plant simulations and scale-up considerations. The pyro-rejuvenator produced after pyrolysis of mining trucks waste tires at 470 °C and distilled between 160 – 200 °C, contains BTX (14.6%), *o*-cymene (10.9%) and limonene (58%), and <10 cP viscosity, which confirms its feasibility for application in asphalt self-healing. Integrated mass balances results in yields of 27 wt.% (pyro-rejuvenator), 11 wt.% heavy fuel, 10 wt.% light fuel and 5 wt.% pyro-gas. The rejuvenator was encapsulated with 97% efficiency within thermochemically stable 1.5 mm alginate-based capsules produced by the vibrating jet method. Environmental Life Cycle Assessment results indicate that water consumption and electricity use during the encapsulation process heavily impact environmental performance, accounting for over 50%, necessitating the exploration of energy integration strategies. Finally, this study demonstrates the feasibility of producing a new generation of asphalt rejuvenators from waste tires sourced from mining trucks.

Keywords: Waste Tires; Pyrolysis; Distillation; Encapsulated Rejuvenator; Life Cycle Assessment.

Graphical Abstract



1. INTRODUCTION

In recent decades, Chile's mining sector has expanded significantly, resulting in substantial economic gains (Cardemil-Winkler, 2020). Nevertheless, this growth has also posed environmental challenges, and one such challenge that has received insufficient attention is the disposal of waste tires from mining trucks. As per the CINC-Chile, an estimated 45,000 tons of tires from mining trucks are disposed of each year, leading to a yearly accumulation of 180,000 tons when combined with tires from other vehicles (Cámara del Neumático en Chile, 2024). Until 2022, only a small portion of these waste tires (about 13%) underwent conventional recycling technologies, while the majority were improperly disposed of (Biblioteca del Congreso Nacional, 2016; Kyklos, 2021).

In this context, pyrolysis has emerged as a promising and effective method for converting the polymeric fraction of tires into gaseous, solid, and liquid by-products. The waste tires (WTs) typically consist of carbon black (~20%), metal (~15%), fabric (~6%), additives (~8%), and elastomers, which include both natural and synthetic rubbers. According to Menares et al., (2020) the pyrolysis temperature and the proportions of natural and synthetic rubbers in WTs plays a significant role in determining the reaction mechanisms during pyrolysis, thereby influencing the distribution of products within the pyro-oils.

Tire pyrolysis oils (TPO) are complex mixtures of hydrocarbons, primarily consisting of aliphatic and aromatic compounds. The TPO features mid viscosity (1.7 to 17.8 cSt), neutral-to-basic pH, a wide carbon number ($C_5 - C_{50}$), and an average H/C ratio of 1.3. The terpenes (limonene), single-ring alkyl aromatics (BTX, *p*-cymene), paraffins (dodecane, tridecane) and some S,O-containing species (thiophenes, cyclopentanone) are among the most abundant compounds in TPO. This diverse chemical nature makes the TPO a homologue to crude oil. Therefore, regardless of its intended application, fine-tuning the composition of TPO is essential for its successful use. This fine-tuning can be achieved through various methods, including control of pyrolysis conditions (e.g., temperature, heating rate, and particle size), use of post-processing techniques (such as distillation and catalytic treatments), or a combination of these approaches (Campuzano et al., 2023; Martínez et al., 2021).

In a recent study Campuzano et al., (2021) demonstrated that the distillation curves for pyro-oils are between those obtained for diesel and gasoline, with hydrocarbon families boiling between 70 °C and 550 °C. Following conventional distillation, the TPO was fractionated into four cuts: light (70 – 176 °C), low-middle (176 – 240 °C), high-middle (240 – 285 °C), and heavy (285 – 550 °C). Structural characterization of these fractions confirmed that aromatics, light alkanes, and alkenes (including terpenes) were concentrated in the light and low-middle fractions, making them suitable for various applications.

While these advancements have been validated at the laboratory and, in some cases, pilot plant scales, most commercial applications of TPO proceed without any upgrading. For example, crude TPO have been utilized as diesel substitute (Martínez et al., 2013), as a solvent and/or additive to heavy oils (Wu et al., 2022), and more recently, as an asphalt rejuvenator for more sustainable self-healing roads (Kumar et al., 2022; Norambuena-Contreras et al., 2021). Despite its potential as a promising solution for producing a new generation of waste-based asphalt rejuvenators, this application has received limited attention in research. In a recent paper, Norambuena-Contreras et al., (2021) demonstrated that crude TPOs features exceptional self-healing properties to restore aged bitumen. Similarly, the same authors demonstrated the high encapsulation efficiency of these pyro-oils into mechanically and thermally stable bio-capsules, which could be further used to prepare asphalt mixtures with enhanced self-healing properties. One hypothesis in Norambuena-Contreras's research is that aromatics and terpenes (e.g., limonene) play a key role in self-healing activity, while other compounds either act as spectators (non-interacting in the process) or hinder the self-healing process, such as acids and heavy PAHs. Their proposal suggests that aromatics help replenish the aromatic/asphaltene ratio in aged asphalt, while light hydrocarbons, limonene, and other terpenes contribute to reconstituting the maltene fraction and providing antioxidant activity. In a more recent paper from the same research group (Chávez-Delgado et al., 2024), it was demonstrated that, after chemical optimization and proper mixing with aged bitumen (at 3–6% weight ratios), pyro-oils produced from a mixture of waste tires improved the viscosity, softening point, and penetration of aged binders, restoring their rheological properties to those of the virgin state.

Additionally, Li et al., (2021) demonstrated that a balanced composition of aromatics and ketones in pyro-oils produced from biomass/tire mixtures promotes the self-healing of bitumen and enhances its mechanical performance after rejuvenation. Thus, to develop an optimized rejuvenator for asphalt self-healing purposes, it is essential to upgrade crude pyrolytic oils by carefully adjusting their composition, focusing on maltenes, aromatics, and antioxidant compounds.

Bitumen, based on its molecular composition, is a viscoelastic, multiphase material with colloidal microstructures, consisting of a solid asphaltene phase and a liquid maltene phase. Bitumen aging occurs due to several environmental factors, including: (i) volatilization of light molecules during asphalt mixture manufacturing at high temperatures (~ 150 °C), (ii) oxidation of hydrocarbon chains leading to the formation of C=O and S=O bonds, and (iii) polymerization during the pavement's service life, catalyzed by environmental conditions (temperature, moisture, UV radiation) and traffic loads. In any scenario, this aging process results in the degradation of the bitumen, leading to a reduction in maltenic and aromatic contents. This decrease in mechanical performance of the asphalt mixture reduces the durability of our roads over time. Therefore, it is essential that asphalt rejuvenation be effective from chemical, mechanical, and temporal perspectives to ensure the prolonged service life of roads.

In this context, encapsulated rejuvenators are recognized as intelligent millimeter-size capsules that impart self-healing capability to asphalt (Concha et al., 2024, 2023). Self-healing occurs when capsules containing asphalt rejuvenators are activated by the formation of microcracks nearby, triggering the release and diffusion of the rejuvenator into the asphalt matrix, thereby enabling autonomous healing (Gonzalez-Torre and Norambuena-Contreras, 2020; Ren et al., 2022). The encapsulation of rejuvenators offers environmental advantages by minimizing the risks linked to the release of harmful compounds, such as alkylbenzenes and toluene, through volatilization during warm pavement preparation or spill-over during direct application. By encapsulating the rejuvenator within the asphalt mixture, rather than applying it directly, the environmental exposure of the oil is reduced, thereby mitigating contamination risks.

Nevertheless, while the development of self-healing asphalt mixtures is a promising area of research, most solutions are still in the early stages of development and lack comprehensive technical and

environmental assessments (Khan et al., 2023). Therefore, there is a lack of information on process scaling and the environmental impacts associated with the production of encapsulated rejuvenators, particularly in terms of a comprehensive Life Cycle Assessment (LCA).

In this study, we conducted technical and environmental analyses on the production of encapsulated pyro-rejuvenators from mining truck waste tires (MTWT). The process includes the production and upgrading of tire pyrolysis oils (TPO) into pyro-rejuvenators, followed by their encapsulation into polynuclear capsules. The analyses incorporated experimental data, modular-sequential modeling, and process synthesis principles. Additionally, the environmental impacts of pyrolysis and encapsulation were quantified using Life Cycle Assessment (LCA) methodology, providing a comprehensive overview of the critical aspects of the technology.

2. MATERIALS AND METHODS

The waste tires from mining trucks, which were used as a case study, were supplied by a local company based in northern Chile. The elemental and proximate compositions of these MTWT are reported in Table S1 (Supplementary material). Additionally, a combination of experimental data, modular-sequential modeling, and declarations of environmental impacts from MTWT pyrolysis plants established in Chile were utilized to analyze the operation and obtain inventory data related to pyro-rejuvenator production (M. Díaz, 2024). In the case of the encapsulation by jet-vibrating technology, the inventory data was obtained from the scaling-up of the processes previously implemented by Concha et al., (2023) and Norambuena-Contreras et al., (2021), which are based on the use of optimized oil-in-water emulsions containing biopolymers from marine biomass, such as sodium alginate. Sodium alginate was selected for encapsulating the rejuvenator due to its non-toxic nature and sustainability, serving as an alternative to commonly used materials such as formaldehyde-based polymers, including Melamine-formaldehyde (MF), Methanol-melamine-formaldehyde (MMF), Urea-Formaldehyde (UF), and Melamine-Urea-Formaldehyde (MUF) (Wan et al., 2022). Moreover, this biopolymer has several advantages when used as encapsulating material for asphalt rejuvenators, such as: I) thermal and mechanical stability as an encapsulating material during the mixing and compaction of asphalt mixtures, and II) the controlled release of rejuvenators, facilitating multiple healing cycles for the

bituminous material (Y. Li et al., 2021). Further details on the encapsulation process modeling and data management are presented in the following sections.

2.1 Processes description

The pyro-rejuvenator is produced through pyrolysis of MTWT, and subsequent pyro-oil refining according to Chávez-Delgado et al., (2024). The process includes a pre-treatment stage to isolate the polymeric fraction of MTWT through washing, shredding, sieving, and steel separation (M. Díaz, 2024). The Process Flow Diagram (PFD) illustrating the production of encapsulated rejuvenators is presented in **Figure 1** and includes three major sections:

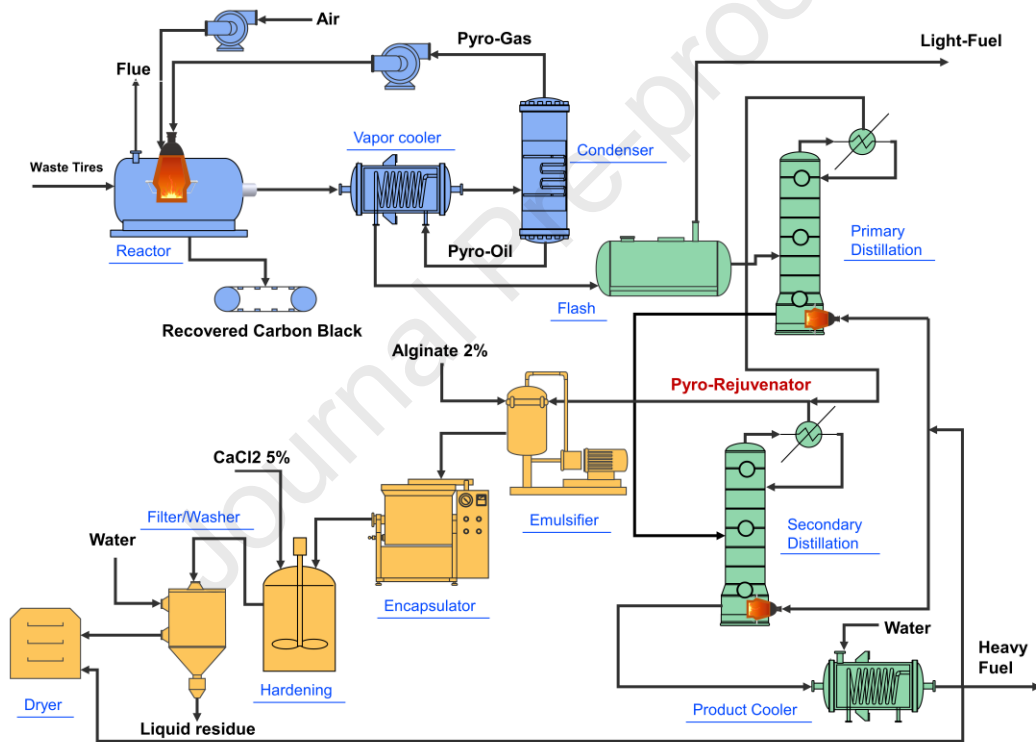


Figure 1. Flow diagram of the waste tire pyrolysis (blue), pyro-oil upgrading (green), and encapsulation of pyro-rejuvenator (yellow).

- The **first section** (devices in blue) includes the pyrolysis reactor, where the thermal decomposition of tires occurs, producing recovered carbon black (rCB), pyro-gas, and pyro-oil. Additionally, this section includes a thermal recovery loop that supplies the necessary heat to the pyrolysis reactor using pyro-gas.

- The **second section** (devices in green) includes an upgrading train to meet the specifications for an asphalt rejuvenator. The system includes a flash drum, two distillation columns, and various coolers and condensers for product conditioning. The energy requirements of the upgrading train are met by burning a portion of the heavy fuel from the bottoms of the secondary distillation column, making the process autothermal overall.
- The **third section** (devices in yellow) outlines the encapsulation of pyro-rejuvenators within polymer-based capsules. Here, we employed an encapsulation by vibrating jet method based on the ionic gelation of alginate in the presence of Ca^{2+} ions (Concha et al., 2023, 2021). The encapsulation process include four stages: (i) preparation of an oil-in water emulsion (O/W) between the pyro-oil rejuvenator and a solution of the encapsulating polymer (here sodium alginate) (Norambuena-Contreras et al., 2022). (ii) Extrusion of the emulsion into a hardening solution (5 wt.% of CaCl_2) through vibration jet technique (iii) Washing and filtering of the capsules, and (iv) drying of the capsules. A schematic of the experimental system utilized for scaling up the four-stage encapsulation process is shown in **Figure 2**.

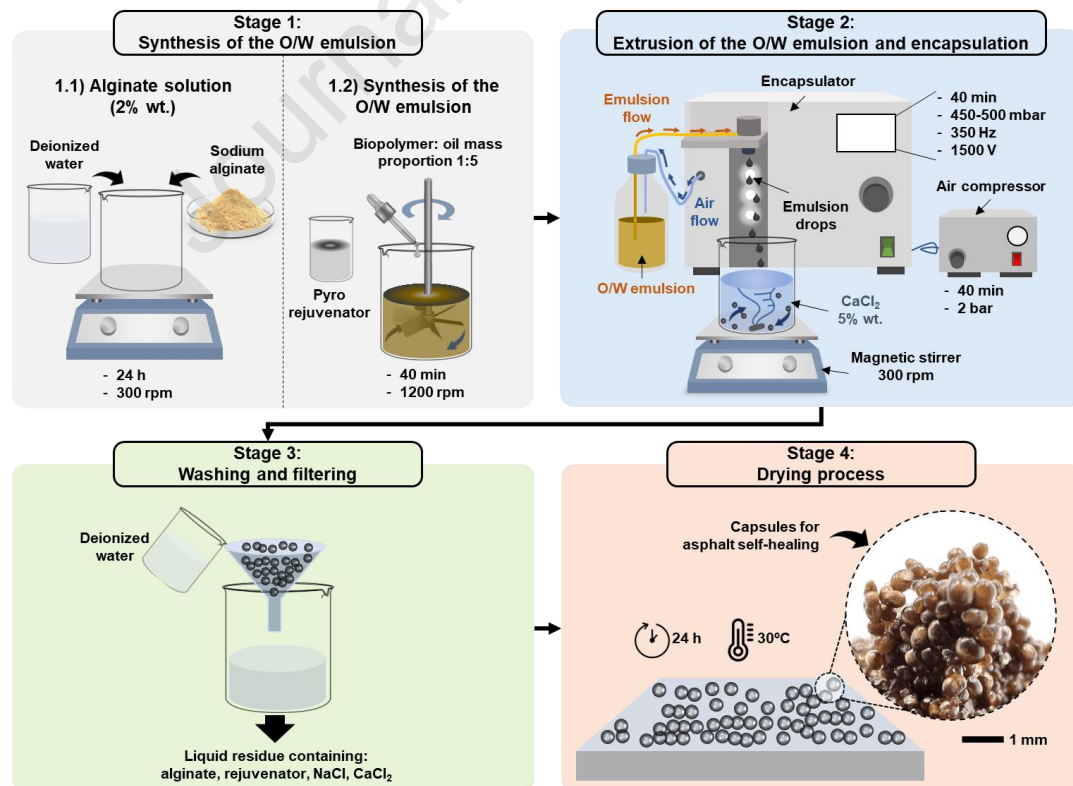


Figure 2. Experimental set-up for the four-stage encapsulation process of the pyro-rejuvenators.

The engineering data for the integrated analysis of these processes was gathered from an Aspen Plus 14.0 simulations, and from traditional scale-up procedures (Larrere, S., 2023; Sinnott and Towler, 2013). The fundamental conditions for plant operation are outlined in Table 1.

Table 1. Process conditions for producing 1000 kg/day of encapsulated pyro-rejuvenators.

Process stage	Process units	Operation conditions	Performance indicators ^a
Waste tire Pyrolysis	Pyrolysis Reactor	400 – 500 °C, 101.325 kPa	Gas Yield ^b (wt.%)
	Gas cooler	70 °C, 101.325 kPa	Solid Yield (wt.%)
	Condenser	Flash separation	Liquid Yield (wt.%)
	Gas Burner	900 °C, 101.325 kPa	Heat recovery (kW _C /kW _P) ^c
Pyro-oil upgrading	Primary Distillation	160/185 °C, 101.325 kPa	Limonene (wt.% in distillate)
			Light fuel yield (wt.%)
	Secondary Distillation	176/200 °C, 101.325 kPa	Distillate/Feed ratio
			Heavy fuel yield (wt.%)
Heavy fuel Burner	900 °C, 101.325 kPa	Rejuvenator yield (wt.%)	
			Distillate/Feed ratio
Encapsulation process	Emulsifier	Biopolymer/Oil:1/5, 700 rpm	Heat recovery (kW _C /kW _D) ^d
	Encapsulator	Nozzle size: 750 μm Frequency: 350 Hz	Creaming Index (>80%)
	Dryer	50 °C, time: 2h	Encapsulation efficiency (>97%)
			Moisture content < 5 wt.%

^aPerformance indicators were defined based on the results obtained under experimental conditions (See sections below).

^bYields are calculated as a function of processed waste tires: $Yield_i = 100 \times (m_i/m_{wt})$, m is mass flow in kg h⁻¹, i is the target product.

^ckW_P and kW_C are the heats required or produced from pyrolysis and combustion of non-condensable gases.

^dkW_D and kW_C are the heats required and produced for distillation and from combustion of light fuel.

2.2 Modeling of pyro-rejuvenator production

The plant models for waste tire pyrolysis were implemented in Aspen Plus v14.0 and validated using experimental data. Details on simulation diagrams are provided in Fig. S1a. The considerations (a-f) used in the modeling are listed below:

- a. All calculations were performed under steady-state conditions to produce 1 ton/day of encapsulated rejuvenator.
- b. Waste tires were defined as a non-conventional solid using the proximate and ultimate compositions reported in Table S1.
- c. Recovered carbon black is represented as a mixture of a conventional solid (graphite) and non-conventional (Ash) (MIXNC).
- d. The thermodynamic properties of conventional products were calculated using the Peng-Robinson equation of state (EOS), while the IGT models for density and enthalpy (HCOALGEN and DCOALIGT) were applied for non-conventional solids.
- e. Air is considered as 79% N₂ and 21% O₂ on a molar basis.
- f. The transformation from non-conventional solids into conventional elements was carried out by a yield reactor, following a procedure reported elsewhere (Rodríguez-Machín et al., 2021).

Section 1: Pyrolysis and Separation

The pyrolysis reactor was modeled using a Heater, a Separator, and two RYield blocks. The first RYield module (YIELD) was integrated with a calculator block for transforming non-conventional waste tires into conventional species (i.e., C, H₂, H₂O, N₂, S, and ashes). Thereafter a heater block (TP-SET) was used to fix the pyrolysis temperature (400 – 500 °C) and to feed a calculator block specifying the yields of recovered carbon black, pyro-gas and pyro-oil from the pyrolysis reactor. Then, a Sep block (SEP) operated under isothermal conditions (same Temperature as the reactor) was used to separate the ashes, and to close the carbon balance between gas/vapor phase and solids. Finally, the chemical compositions of pyro-gas and pyro-oil were predicted in the second RYield module (REACTOR), using temperature-dependent correlations that replicate experimental results (Tables S3 to S5). After that, the products from the reactor

(vapor and non-condensable gases) are separated in an isobaric condenser, simulated here by a Flash2 block (COND). The condenser temperature is controlled by a Design Spec tool, which guarantee the closure of the mass balance between model and experimental results. The pyro-oil obtained in the condenser is preheated by cooling-down the reactor products in a HeatX block (HREC) to reduce the utilities demand in the system. The heat recovery loop for pyrolysis is simulated by using a RGibbs (900 °C and 1 atm), and a Heater block (COMB and QCOMB) module. The flue gas temperature from this loop was set at 150 °C to avoid condensation in the stack. The air flow entering the combustion chamber was adjusted to match the temperature and to guarantee that the exit gas's oxygen concentration was below 5% v/v. The heat balance in the pyrolysis section was checked by a Q-Mixer block (Q-LOSS), including all heat sources and sinks, and with an efficiency penalty of 10% (Wu et al., 2022).

Section 2: Pyro-oils upgrading for producing pyro-rejuvenators

The crude pyro-oil enters the upgrading section to be fractionated into three distillation cuts: <160 °C, 160 – 200 °C, and >200 °C, respectively. The product distribution between the cuts was compared to that obtained in an experimental batch distillation system, like that reported in Campuzano et al., (2021b). The first separation was achieved by flashing the pyro-oil at 160 °C in a Flash2 block (FLASH), the top product from this block is the light fuel (LFUEL-1), while the bottom enters a RadFrac distillation unit (PRIMARY) leading to the separation of the second cut. The tops of the primary and secondary distillations were mixed at 20 °C to yield the pyro-rejuvenator (REJ). The water consumption in all cooling and condensation stages was calculated by Design specification and HeatX blocks (COND-LF, COND-REJ, HF-COOL). Finally, the heat demand from the distillation columns is fulfilled by using a fraction of heavy fuel in a second heat recovery loop. The simulation of this loop followed the same principles previously described for the heat recovery from pyro-gas. Here, we applied an additional design specification to calculate the flow of heavy fuel required to maintain the energy balance within the pyro-rejuvenator production and the drying of capsules in the downstream encapsulation system. The process simulation diagram of the previously described waste tire pyrolysis plant, along with a comprehensive specification of Aspen Plus's modeling blocks, is available in the supplementary material. (see Figs. S1A and S1B, and Table S2).

Section 3: Encapsulation of pyro-rejuvenators

The encapsulation process starts with the preparation of an O/W emulsion, using a 2 wt.% sodium alginate biopolymer solution and the pyro-rejuvenator, Figure 2. The emulsion is obtained by mixing the oil and the biopolymer at a mass ratio of 5:1 and stirring at 950 rpm (Concha et al., 2021). Once the emulsion is prepared, the second step involves the formation of alginate-based capsules using the vibrating jet technique with a Buchi B-390 encapsulated (Flawil, Switzerland). This involves pumping the freshly prepared emulsion through a 750 μm nozzle attached to a vibrating unit operating at a frequency of 350 Hz. These parameters enable the extrusion of the emulsion in laminar flow, resulting in the formation of uniformly distributed droplets due to vibration. An electrostatic charge of 1500 V is applied to the droplets during the process to prevent agglomeration. Finally, the droplets are collected in a 5 wt.% CaCl_2 hardening solution, which is stirred at 250 rpm. In the third step, the capsules are filtered from the hardening solution, washed with process water to remove any residual impurities, and then placed in a tray dryer operating at 50 °C for 2 hours. Once fully dried, the capsules are cooled to an ambient temperature and stored. This process was scaled-up to produce 1.0 ton/day of capsules, by using several factors (constant Reynolds, constant agitation speed, known air-drying kinetics, constant power numbers, etc.) (Larrere, S., 2023; Sinnott and Towler, 2013). Major performance indicators are reported in Table 2.

Table 2. Performance indicators for the encapsulation of pyro-rejuvenator in capsules.

Parameter	UM	Value
Water consumption*	kg/kg _c	12.8
Encapsulation efficiency	%	97
Sodium Alginate ($\text{NaC}_6\text{H}_7\text{O}_6$) _n	kg/kg _c	0.18
CaCl_2 consumption	kg/kg _c	0.05
Oil:Polymer mass ratio	a.u.	5:1

*kg_c refers to 1 kg of capsules.

**Gelation reaction: $2(\text{NaC}_6\text{H}_7\text{O}_6) + \text{CaCl}_2 \rightarrow (\text{C}_{12}\text{H}_{14}\text{CaO}_{12}) + 2 \text{NaCl}$

2.3 Data availability and model validation for pyrolysis

The experimental data used for validating the pyrolysis models was obtained from a custom-designed plant (see Fig. S2). In a typical experiment, about 4 kg of waste tires (size 1 – 2 mm) were fed into a cylindrical reactor (ID: 21 cm and H: 41 cm) equipped with a stirrer (200 rpm) and with three K-type thermocouples to guarantee a uniform internal temperature profile. The pyrolysis temperature varied between 400 °C and 500 °C, and the system was operated under a constant N₂ flow (1 – 2 L/min). The pyrolysis vapors were collected downstream the reactor in a water-cooled condenser (15 °C), while the non-condensable gases were analyzed using a portable analyzer (ETG MCA 100 Syn-P), then washed and flared.

Distillation curves at atmospheric pressure were recorded for pyro-oils produced at different temperatures, following the ASTM D 86 standard (ASTM D86-23, 2024) (Fig. S3). For the assay, 200 mL of pyro-oil were placed in a round bottomed flask, equipped with a mechanical stirrer (200 rpm). The liquid was then gradually heated from room temperature (15 °C) to 280 °C using a heating mantle. The temperature was controlled using two K-type thermocouples placed inside the distillation mixture and at the vapor outlet, respectively. As the temperature increased, condensed vapors were collected, and the volume fractions of the distillate were recorded as a function of temperature. Each cut underwent characterization for chemical composition analysis using gas chromatography coupled to a mass spectrometer (GC-2010 Plus, Shimadzu and QP 2010 Ultra, Shimadzu).

The selection of the pyrolysis conditions and the distillation cut to produce the pyro-rejuvenator will depend on the pyro-oil yield and composition. In particular, the analysis aims to maximize the content of aromatics and alkenes, as the self-healing effectiveness of the rejuvenator for asphalt applications heavily depends on these substances (C. Li et al., 2021; Norambuena-Contreras et al., 2021).

2.4 Life Cycle Assessment

The Life Cycle Assessment (LCA) of the integrated processes described in the preceding sections was carried out by following the ISO 14044 guidelines (ISO, 2006). The LCA was performed in the SimaPro v8.5.2 software using the hierarchy version of the ReCiPe 2016 midpoint method. The impact categories

included in this method were: Global warming (GW), stratospheric ozone depletion (SOD), ionizing radiation (IR), ozone formation human health (OFHH), fine particulate matter formation (FPM), ozone formation terrestrial ecosystems (OFTE), fresh water eutrophication (FWEU), marine eutrophication (MEP), terrestrial ecotoxicity (TET), fresh water ecotoxicity (FWET), marine ecotoxicity (MET), human carcinogenic toxicity (HCT), human non-carcinogenic toxicity (HNCT), land use (LU), mineral resources scarcity (MRS), fossil resources scarcity (FRS), fresh water scarcity (FWS) and water consumption (WCO).

2.4.1 Goal and scope definition

This study aims to quantify the potential environmental impacts associated with the production of encapsulated pyro-rejuvenators for their subsequent application for asphalt self-healing.

2.4.2 System boundaries and functional unit

The quantification of the environmental impacts associated with the production of encapsulated pyro-rejuvenators was conducted by considering one kilogram (kg) of capsules as the functional unit (FU). The system boundaries for the supply chain of encapsulated pyro-rejuvenators were defined considering a “cradle to gate” scenario (Fig. 3). This scenario includes a *Foreground System* with five stages: (i) transportation of MTWT, (ii) MTWT pre-treatment, (iii) MTWT pyrolysis, (iv) rejuvenator production, and (v) the encapsulation process. In this system, the pyro-rejuvenator serves as the primary material.

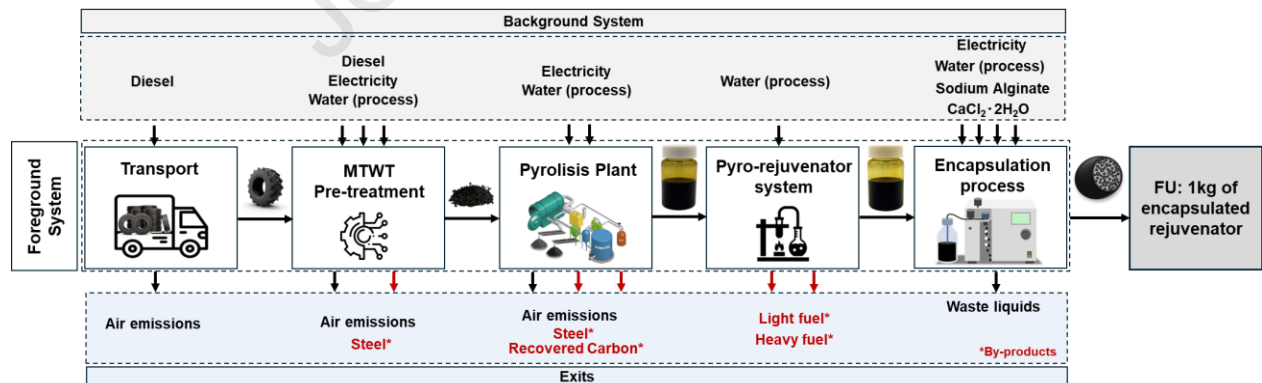


Figure 3. System boundaries to produce encapsulated pyro-rejuvenators from waste tires coming from the mining industry (MTWT: mining truck waste tires, and FU: Functional Unit).

The principal system for pyro-rejuvenator production is supported by a *background system* which considers the production of diesel, treated water (i.e., deionized, distilled or process water), sodium alginate, CaCl_2 , and electricity. Furthermore, this system includes the management of the liquid wastes generated during the encapsulation process. Beyond these systems, the emissions and co-products that arise during all stages of the process are considered. Below is a brief description of the system's inputs and outputs, along with the considerations for the Life Cycle Assessment (LCA):

Stage-i) Transport of MTWT: Consider the transportation of waste tires from the mines to the pyro-rejuvenator production plant, utilizing trucks with a capacity ranging from 7 to 16 tons. The transportation distance was determined to be approximately 123 kilometers, considering the specific location of an MTWT pyrolysis plant (-23.73746, -70.30071), and the mines as reported by the Chilean Mining Council in 2023.

Stage-ii) MTWT pre-treatment: It involves the handling and pre-treatment (i.e., disassembly, cutting, crushing and separation) of MTWT fractions, prior to the pyrolysis plant. The inputs utilized for the handling equipment include diesel fuel, while for the pre-treatment processes, the primary inputs consist of MTWTs, water, and electricity. The main product from this stage is the crushed rubber from MTWT, and steel as a by-product.

Stage-iii) Pyrolysis: This stage involves the thermochemical transformation of the feedstock (crushed rubber from MTWT) into three products: tire pyrolysis oil (TPO), tire pyrolysis gas (TPG) and the recovered carbon black (rCB). Here the pyro-oil is considered as the main product, while the carbon black is a co-product. Finally, the gaseous product is burned in a heat recovery loop to provide the thermal energy required by the pyrolysis, while emitting exhaust gases to the atmosphere.

Stage-iv) Production of pyro-rejuvenator: The production of the pyro-rejuvenator is carried out by three separation stages, involving a primary flashing followed by two distillations processes. The feedstock to this process is the TPO produced in the pyrolysis, while the pyro-rejuvenator is the main product. Moreover, a light and heavy fuel by-products are obtained and considered as substitutes for fuel oil and diesel, respectively. A fraction of the heavy fuel is burned to provide the thermal energy required by the distillation units and drying, thus the exhaust gas stream from this combustion is included in the analysis.

Moreover, after fulfilling the system heat balance the surplus light and heavy fuels are considered as by-products.

Stage-v) Encapsulation: The main feedstocks to the encapsulation process are the pyro-rejuvenator, the sodium alginate, and the calcium chloride. Moreover, this process consumes demineralized water, process water and electricity for the preparation of the O/W emulsion, hardening solution and drying.

2.4.3 Allocation Principles

The allocation principle is applied to multifunctional products processes. According to the ISO 14044 (ISO, 2006), wherever possible, the allocation should be avoided by expanding the system and considering the by-products as substitutes to homologue products in the market. Such a consideration is conceptualized as “avoided products”. When an allocation cannot be avoided, the partitioning must be carried out by physical properties (i.e., mass, energy, exergy, and economy) (Dewulf and Van Langenhove, 2005; Jungbluth and Frischknecht, 2006). The main assumptions considered for this analysis are listed below:

- In this study, no allocation rules were applied to the transportation of MTWT.
- The NTWT pre-treatment phase is treated as a multi-product process, with crushed rubber as the primary product and steel as the by-product. Therefore, based on mass flows reported in M. Díaz, (2024) the contribution of primary product and by-product was defined as 83% and 17%, respectively.
- In the pyrolysis stage, we employed a mass flow-based approach to distribute the allocation loads. The primary product, pyro-oil, accounted for 57%, whereas the by-products steel and recovered carbon black represented 0.1% and 42.9%, respectively.
- In the pyro-rejuvenator production stage, the main product is the pyro-rejuvenator, accounting for 53%, and by-products "light fuel" and "heavy fuel" represent 15% and 32%, respectively.
- Finally, the environmental impacts associated with plant construction and dismantling were omitted from the analysis due to insufficiently reliable information.

2.4.4 Life Cycle Inventory

The inventory data for the *Foreground System* was gathered from different sources, including data for the pretreatment stage was obtained from the environmental product declaration of an existing tire

pretreatment plant (M. Díaz, 2024). The data for the pyrolysis plant and pyro-rejuvenator production was obtained from the simulation model described in the preceding sections. Finally, the inventory for the encapsulation process was obtained after the scaling up of the technology.

For the *Background System*, the data specifically for diesel, process water, deionized water, $\text{CaCl}_2 \cdot 2\text{H}_2\text{O}$, and electricity was sourced from the Ecoinvent v2.1 database. This database also provided information regarding the waste treatment and atmospheric emissions resulting from diesel combustion. The impacts of MTWT transportation were estimated using specific emission factors also provided by this database. The electricity system was modeled using power plants datasets available in Ecoinvent, taking as bases the Chilean electricity matrix configuration for 2022 (Comisión Nacional de Energía, 2022). The wastewater treatment inventory was gathered following local practices, which involved the activated sludge technologies coupled with sludge treatment via anaerobic digestion for obtaining a stabilized sludge and its further application on agriculture or forestry lands (Cartes et al., 2018).

3. RESULTS AND DISCUSSION

3.1 Simulation results

3.1.1 Pyrolysis

The experimental results obtained from the pyrolysis of MTWT were accurately predicted by the simulation model, as evidenced by the agreement between calculated and measured yields of the gas, solid, and liquid fractions (Fig. 4a), with an $R^2 > 98\%$. This successful prediction validates the model's ability to increase the operational region to determine the more feasible conditions to produce pyro-rejuvenators at the industrial-scale. When the pyrolysis temperature increased from 400 to 500 °C, the yield of recovered carbon black (solid) decreased, indicating that higher temperatures promote the conversion of polymers into fluid phases (Fig. 4b). Notably, the yield obtained at 500 °C (38 wt.%) for the solid fraction was similar to that determined through previous thermogravimetric analysis of MTWT (not shown here), indicating that depolymerization was complete. Furthermore, the increase in the pyro-oil's mass yield upon 460 °C supports the previous hypothesis, while its slight reduction thereof confirms the occurrence of secondary and tertiary reactions between 480 and 500 °C. These secondary reactions could lead to the formation of

heavier aromatic compounds, such as tri-aromatics, tetra-aromatics and penta-aromatics, which could reduce the effectivity of the pyro-rejuvenator to promote self-healing processes (Campuzano et al., 2023, 2020; C. Li et al., 2021; Osorio-Vargas et al., 2021).

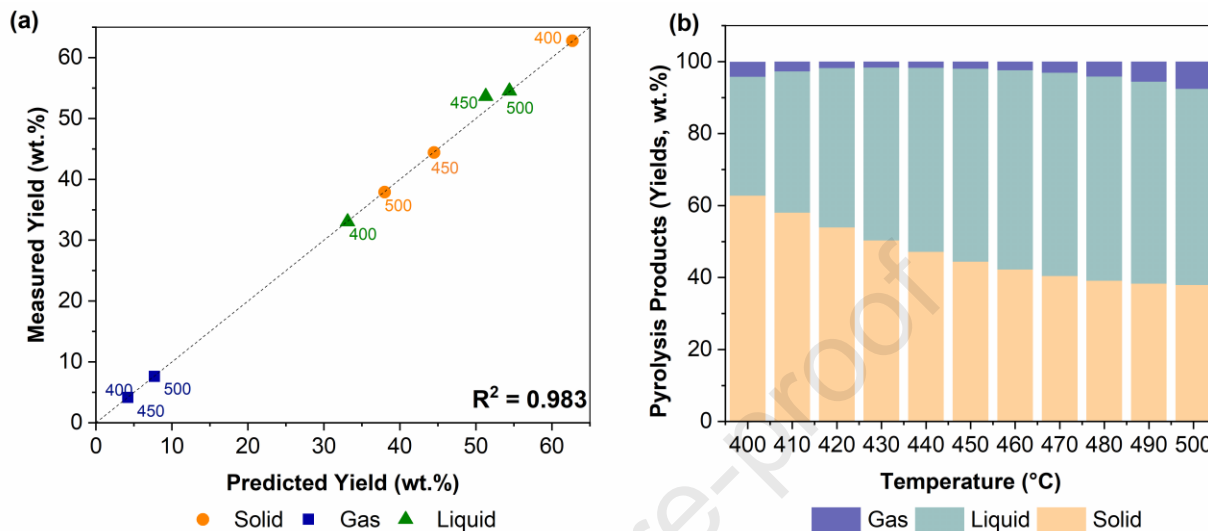


Figure 4. Simulation results and model validation for MTWT pyrolysis; (a) Effect of temperature on the predicted pyrolysis yields; (b) Parity plot between predicted and measured yields for gas, liquid and solid fractions from MTWT pyrolysis. Graph data can be gathered from Tables S3 to S5.

The observed behavior in mass yields can be attributed to the high polyisoprene content in the rubber fraction of MTWT, estimated to be approximately 75%. In our previous research, we discovered that polyisoprene undergoes a multi-step reaction mechanism involving unzipping, cyclization, and intramolecular scissions upon thermal conversion up to 480 °C (Menares et al., 2020; Osorio-Vargas et al., 2021). Indeed, several studies have confirmed that the primary reactions responsible for polyisoprene conversion occur between 400 and 440 °C, producing crude pyro-oils enriched with limonene, isoprene, and single-ring aromatics. Subsequently, at higher temperatures (450 – 480 °C), secondary isomerization and dehydrogenation reactions of limonene occur, leading to an increase in the yield of aromatics. However, further increases in temperature promote aromatization reactions while also inducing the formation of

heavier molecules, such as polyaromatics, thiophenes, and long-chain hydrocarbons. Additionally, higher temperatures raise the energy demands of the pyrolysis process, thereby affecting its thermal balance.

3.1.2 Upgrading of pyro-oil by distillation

The experimental distillation curves and yields of the Light ($T < 160$ °C), Middle (160 °C $< T < 200$ °C) and Heavy (> 200 °C) cuts for pyro-oils produced at 400 °C, 450 °C and 500 °C are shown in Fig. 5a-b. Results confirmed that the three pyro-oils start evaporating at approximately 60 °C and featured a similar trend with 71.5% , 77% and 86.5% cumulative distillate's yields at 280 °C for pyro-oils obtained at 400 , 450 and 500 °C, respectively. Moreover, at the boiling point of the middle fraction (here cut at 200 °C) the recovered distillate was between 40 and 50% , which suggest that the valorization of this fraction should include a commercial solution for the heavier one. In addition, the yields for the distilled fractions (Fig. 5b) changed with the pyrolysis temperature, which could be explained by the reaction sequence previously discussed, where secondary and tertiary reactions occurring at higher temperatures led to heavier pyro-oils. Despite these fraction's yields are critical, the decision on what cut utilize to produce pyro-rejuvenators relies on the chemical composition and physical properties of the cuts. To unravel this question, Campuzano et al., (2021b) recommended a complete structural characterization of distillation fractions; thus here we correlated the GC/MS analysis of the cuts through mathematical modelling to inspect the presence of chemicals with rejuvenation potential.

The results (Tables S6a-d) confirmed that limonene and aromatics (*i.e.*, benzene, toluene, o-xylene and *p*-cymene) were the most abundant species within the middle cut ($> 60\%$), regardless of the pyrolysis temperature. Moreover, the heavy distillation cut featured more than 15% of polyaromatics and 23% of C_{+30} and S-containing products, with an average molecular weight of 160 kg/kmol. Finally, the light cut (< 160 °C) was enriched in single-ring alkylaromatics ($33 - 39\%$), limonene ($32 - 35\%$) and light olefins ($7 - 12\%$), which lead to a molecular weight of $107 - 108$ kg/kmol.

Based on the composition, and boiling points of the three cuts, we concluded that the middle fraction from pyro-oil's distillation can be used as a pyro-rejuvenator. This pyro-rejuvenator will contain a high

share of aromatics and limonene, conferring it a solvent and antioxidant character, which could improve the self-healing properties of the asphalt pavements.

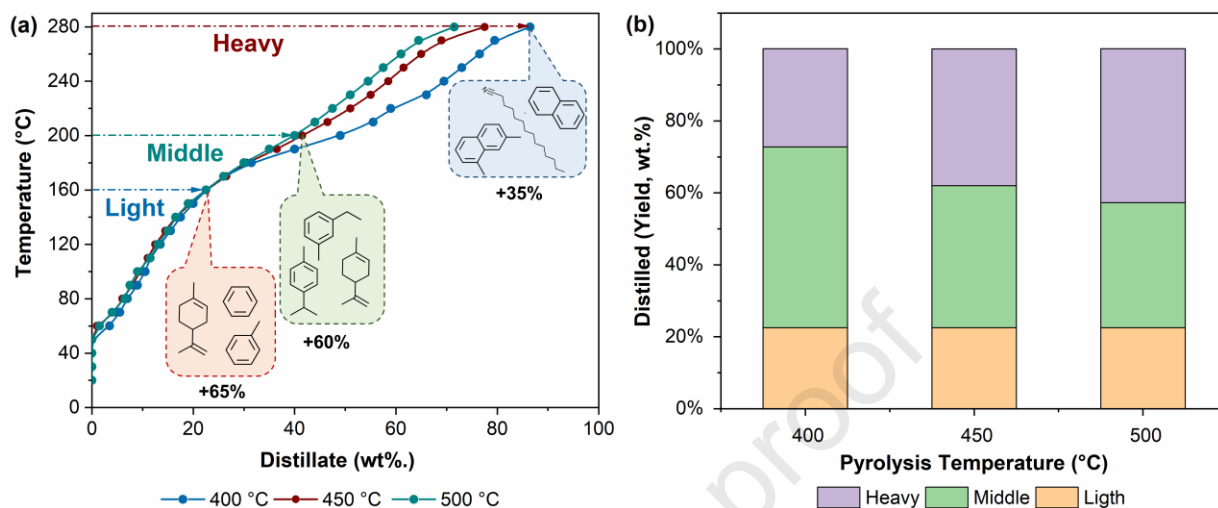


Figure 5. (a) Distillation curves and yields (insert) measured for pyro-oils produced at 400, 450 and 500 °C, (b) Yields and composition of distillation fractions. For a full characterization refer to Tables S6 to Table S7a – S7c.

Conversely, the light fraction was discarded as most of the asphalt pavements are prepared at temperatures above 160 °C, while the heaviest cut could exhibit a poor rejuvenating capacity due to its high viscosity, PAHs, C_{+30} and Sulfur contents. This fraction could also contain asphaltenes and other heavier compounds which were impossible to detect by GC/MS. Hence, both the light and heavy fractions will be regarded as fuels for the process evaluation and life cycle assessment.

After the analysis of the experimental results, the pyro-oil upgrading train was simulated. The results in Fig. 6a shows the yields of the simulated distillation fractions, along with the pyro-oil yield obtained at pyrolysis temperatures between 400 and 500 °C. The simulations reveal a significant phenomenon: within the temperature range of 470–490 °C, the pyro-oil yield reaches its maximum, corresponding to a plateau observed in the distillation curves. These results suggest that the composition of the distilled fractions within this temperature range remains relatively consistent, with only minor de-alkylation and/or

aromatization occurring. Therefore, based on these results, a feasible operation point at 470 °C was defined to reduce the energy consumption during pyrolysis while simultaneously maximizing the yield of pyro-oil.

Finally, the pyro-rejuvenator produced under these conditions contains a high share of BTX (14.6%), *o*-cymene (10.9%) and limonene (58%), which according to our previous results indicates its feasibility for asphalt self-healing (Fig. 6b). A summary of the composition and physical properties of the three major products from MTWT pyrolysis and further pyro-oil distillation is presented in Table 3.

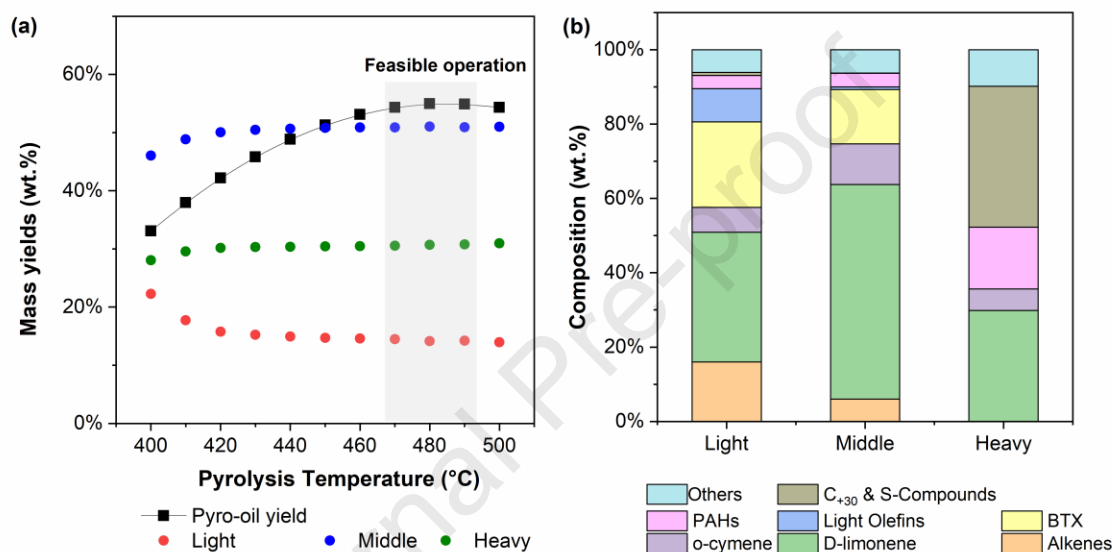


Figure 6. (a) Simulated pyro-oil yield and distillation fractions and (b) chemical composition of the distilled fractions for a pyro-oil produced at 470 °C.

Moreover, the identity of aromatic species in the light fuel and rejuvenator are similar, although the proportions of such chemical identities within these fractions are distributed differently. For instance, light fuel contains nearly 22% of light aromatics (toluene, ethylbenzene, and *o*-xylene), while for the rejuvenator this percentage is reduced by 40%. As well, the rejuvenator features ~1.6 times higher content of limonene and *o*-cymene than the light fuel, thus confirming its potential for asphalt self-healing applications.

The ageing process of bitumen involves oxidation, volatilization of lighter substances, steric hardening of resins, and exudation of oils, including saturates and aromatic components. These chemical transformations result in asphaltene clustering, accompanied by a reduction in the maltene fraction, which ultimately leads to a loss of dispersion within the colloidal bitumen system. The application of a pyro-

rejuvenator containing a high concentration of aromatic and antioxidant compounds such as BTX, *o*-cymene, and limonene would facilitate the redispersion of the colloidal system by adjusting the composition of Saturates, Aromatics, Resins, and Asphaltenes (SARA) in the bitumen. The diffusion of limonene and *o*-cymene within bitumen effectively reduces the fraction of C=O and S=O containing groups through intramolecular interactions, thereby enhancing the antioxidant capacity of the bitumen (Quezada et al., 2024). Therefore, given its potential effectiveness for asphalt self-healing applications, the process conditions used to produce the pyro-rejuvenator, as detailed in Table 3, were used as a reference to evaluate the mass and energy balances associated with its encapsulation in bio-polymeric capsules.

Table 3. Properties and detailed composition of the pyrolysis-distillation products after Aspen Plus simulation. $T_p = 470$ °C. A full list of compounds can be found in Table S6c.

Properties	Units	Light Fraction	Middle fraction	Heavy Fraction
		(Light Fuel)	(Rejuvenator)	(Heavy Fuel)
Viscosity	cP	0.60	1.04 (1.77)*	3.80
Mass Density	kg/m ³	468.2	839.6 (868)*	825.3
Yield	wt.%	14%	51%	31%
Average MW	kg/kmol	104.3	126.1	160.3
Composition (wt.%)				
Alkenes	%	15.99	6.04	0.00
limonene	%	34.94	57.70	29.84
<i>o</i> -cymene	%	6.67	10.93	5.83
BTX	%	22.97	14.59	0.00
Olefins	%	8.97	0.76	0.00
PAHs	%	3.53	3.64	16.60
C+30 & S-compounds	%	0.84	0.05	37.87
Other	%	6.09	6.30	9.85

* Values between brackets were measured experimentally. See (Chávez-Delgado et al., 2024).

3.1.3 Integrated mass and energy balances for pyro-rejuvenator production

The results for the mass balances in the integrated pyrolysis-distillation-encapsulation processes are reported in Fig. 7 for a total capacity of 1000 kg/day of encapsulated rejuvenator. The calculations were performed by integrating the results from Tables 2 and 3.

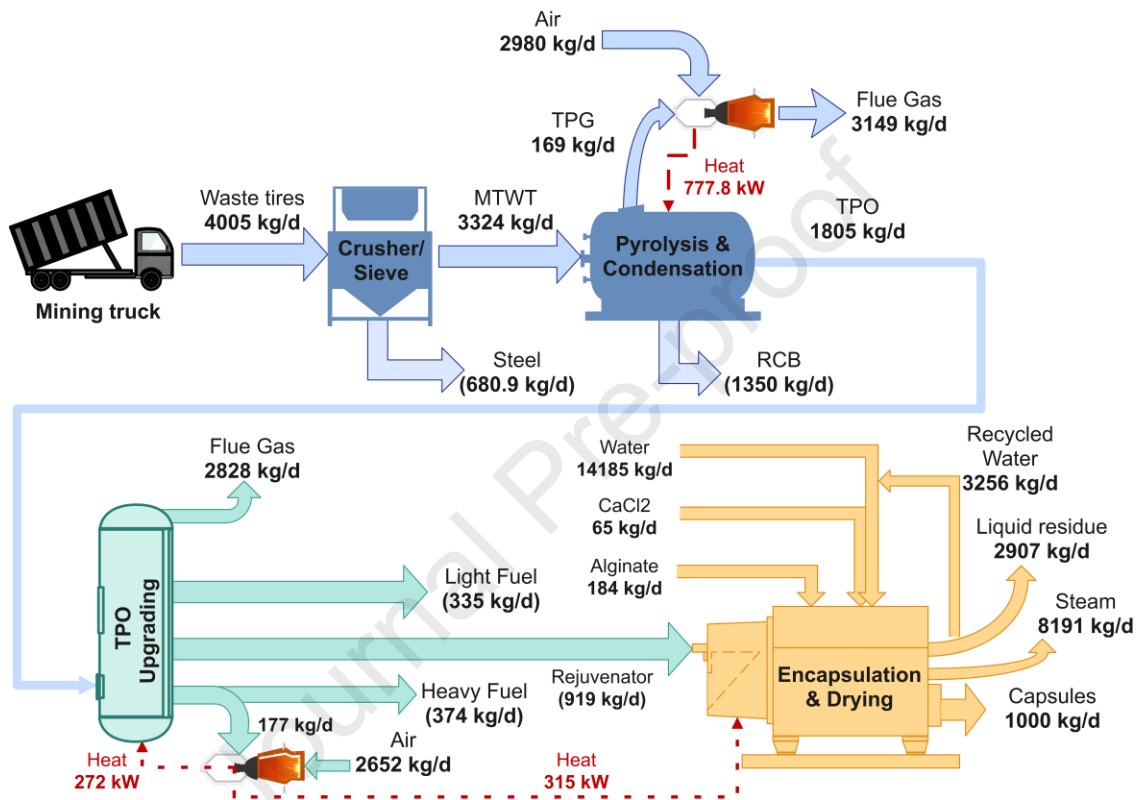


Figure 7. Results of mass and energy balances for producing encapsulated pyro-rejuvenators. $T_p = 470$ °C, Rejuvenator obtained from distillation cut at 160 – 200 °C.

The yield of pyrolysis products was distributed as 27.6 wt.% (pyro-rejuvenator), 11.2 wt.% heavy fuel, 10 wt.% light fuel and 5% gas. Moreover, a 40.6 wt.% of the MTWT feed into the pyrolysis system is recovered as recycled carbon black, which could be applied as additive in the preparation of asphalt mixtures (Martínez et al., 2019). Finally, a 32 wt.% of the heavy fuel was used as energy source to fulfill the heat requirements of TPO distillation and capsule's drying, while the pyro-gas was completely burned

resulting in an autothermal process. Likewise, about 3.3 m³ of water are recycled to the encapsulation process (for emulsion preparation), to reduce the freshwater use and the water treatment requirements by 80% and 66%, respectively. The liquid residue is an aqueous solution of 0.78 wt.% pyro-rejuvenator, 0.11 wt.% CaCl₂, 1.19 wt.% NaCl and 1.3 wt.% (NaC₆H₇O₆ + C₁₂H₁₄CaO₁₂), thus it should be treated prior to its disposition. Finally, the composition of exhaust gases from pyro-gas and light fuel combustion are reported in Table S7.

The total emissions from the process were calculated using the Aspen Plus v14 CO₂ estimator (Scope 1, excluding utilities). From this analysis, the streams with the highest CO₂ contribution were the exhaust gases from the heat recovery loops (summing 99.5% of the whole emissions), while the difference (about 0.5%) was distributed between rejuvenator, light, and heavy fuels (Fig. S4). The results from these integrated balances will be used in subsequent sections to quantify the environmental impacts of producing 1 ton of encapsulated pyro-rejuvenators through a Life Cycle Assessment approach.

3.2 Life Cycle Analysis (LCA)

3.2.1 Environmental impacts of production and encapsulation of pyro-rejuvenators

The environmental profile of 1 ton of encapsulated pyro-rejuvenators disaggregated by life cycle stage is depicted in Fig. 8. The encapsulation process presents the highest environmental burdens for most impact categories (36 – 97%), except for terrestrial ecotoxicity (29%). Specifically for terrestrial ecotoxicity, waste tire transport is the most relevant stage, representing 63% of the total impact due to air and water emissions generated during oil crude refining for diesel production. This also constitute the main causes of the impacts on freshwater (25%) and marine eco-toxicities (44%) reported for transport. Besides, pre-treatment contributes to 4 – 13 % of global impacts due to diesel-based handling machinery that carries the waste tires from the collection to the dismantling process. The CO₂ emissions derived from syngas combustion in the pyrolysis heat recovery loop, have a 21% share of the global warming category. In contrast, the process of upgrading crude oil into a pyro-rejuvenator (which includes flash and distillation stages) shows negligible impacts. This is due to the low air emissions associated with the combustion of heavy fuel, used to meet the heating demand for the TPO upgrading process (272 kWh).

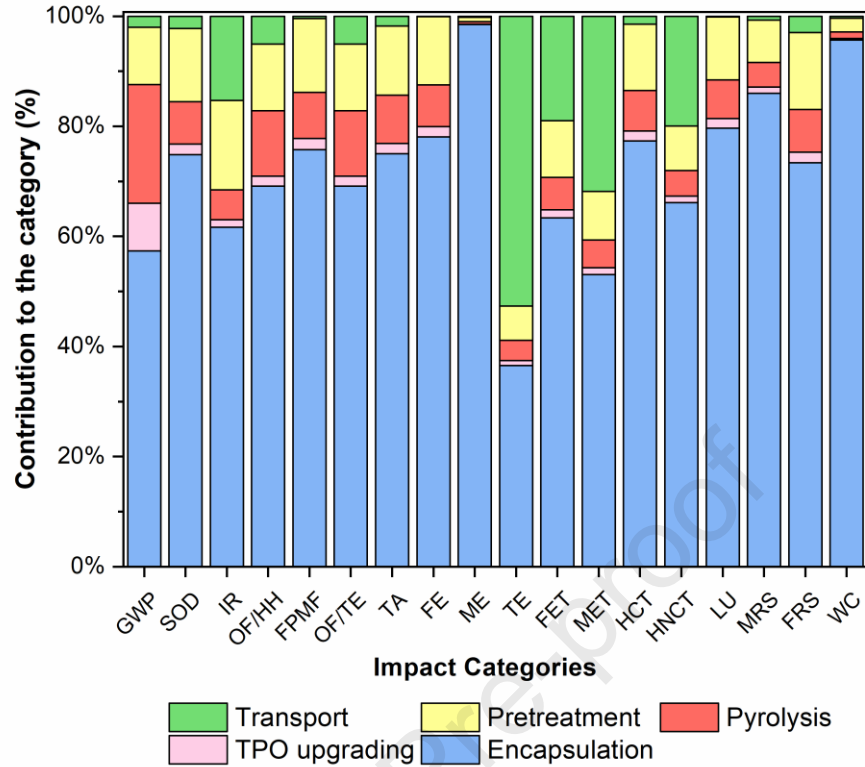


Figure 8. Environmental impacts of the production of encapsulated rejuvenators from upgraded TPO from the ReCiPe 2016 midpoint hierarchist (H) method.

The prevalence of the encapsulation stage can be explained by high electricity demand and the Chilean electricity matrix structure as it is shown in Fig. 9. Specifically, this stage consumes 52% of the total process electricity demand, being the capsule drying (48% of the total encapsulation stage), vibrational-spraying encapsulation technique (28%) and agitation systems required for emulsion formation (23%) the main contributors. Additionally, the production of calcium chloride significantly affects the mineral resources category (40%) and land use category (27%) of the total impact of the encapsulation process. This impact is closely linked to limestone extraction.

The coal share in the Chilean electricity matrix represents a 23% (Energía Abierta, 2023); consequently, coal extraction and its combustion contribute significantly to the environmental burden associated to the encapsulation. These findings underscore the need to decrease our process's reliance on national energy matrix. In this scenario, the environmental footprint of encapsulation could be substantially reduced by

adopting cleaner electricity production systems or by integrating materials and energy utilities directly into the process. For instance, the light and heavy fuel fractions coming from TPO upgrading have good fuel properties in terms of heating value (avg. 41.75 – 47.7 MJ/kg) and a low amount of sulfur (<100 ppm), hence they can be used as energy sources to produce heat and electricity (Pourhashem et al., 2013).

In this context, various energy improvement strategies could be explored, including: (i) replacing electric dryers with thermal ones, and (ii) doing the same replacement integrated with an internal combustion engine (ICE) to generate the electricity required by the process (Arteaga-Pérez et al., 2014; François et al., 2013).

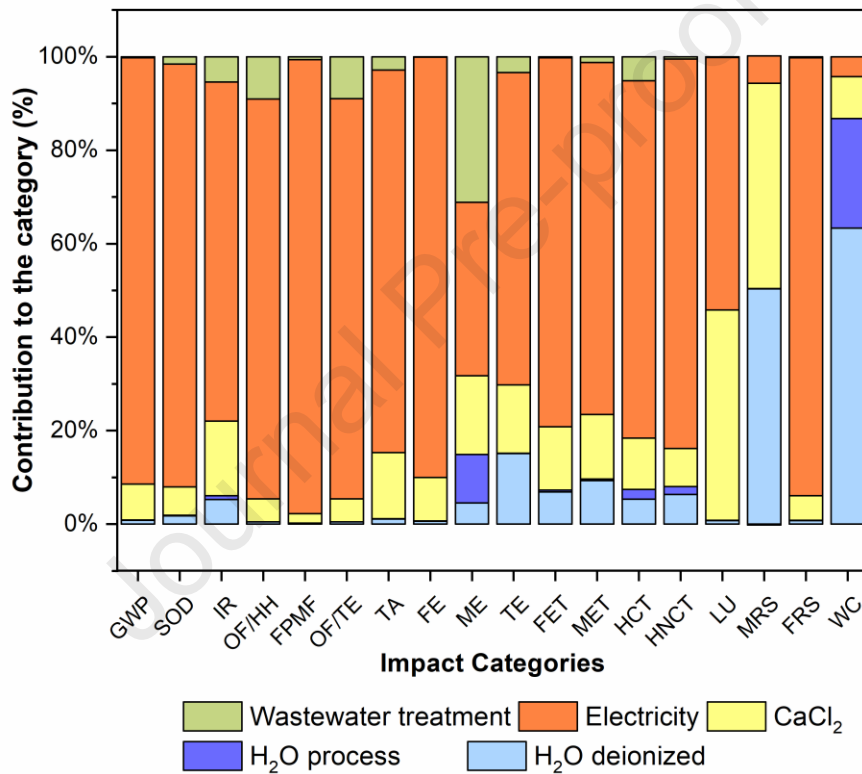


Figure 9. Environmental impacts associated to the encapsulation of pyro-rejuvenators into alginate-based capsules. The impact categories correspond to the ReCiPe 2016 midpoint hierarchist (H) method.

3.2.2 Environmental implications of drying and energy management

Table 4 illustrates the environmental performance of the scenarios (i) and (ii) described previously. The findings show that the utilization of a thermal dryer and an integrated thermal dryer-ICE system leads to a reduction in reliance on the national electricity mix by 27% and 82%, respectively. Consequently, a

substantially improved environmental performance across nearly all impact categories is observed compared to the electric dryer alternative. Particularly noteworthy is the decrease in fossil resource scarcity by 36-79%, resulting in a corresponding reduction in the environmental impact associated with their extraction and combustion during electricity generation, encompassing ecotoxicities, eutrophication, human toxicities, land use, water consumption, and mineral scarcity.

On the contrary, the combustion of partial or total heavy and light oil from TPO results in a notable increase in carbon emissions due to the hydrocarbon mixtures present in the oil fractions (refer to Table 3). As a result, global warming increases by 14% for the thermal dryer and 158% for the thermal dryer-ICE when compared to the electric dryer. These substantial variations among scenarios can be attributed to the extent of electricity replacement by pyro-oil combustion.

Furthermore, the thermal dryer coupled with an internal combustion engine exhibits higher impacts in specific critical categories compared to other scenarios, notably global warming, ozone formation, acidification, freshwater eutrophication, and terrestrial ecotoxicity. This observed trend arises from the replacement of not only 44% of fossil fuels (23% coal, 10% natural gas, and 9% liquefied natural gas) used in the national electrical grid but also electricity sourced from renewable energy (57%). In this context, the combustion of light and heavy oils proves to be more environmentally harmful than the natural gas used in the national electrical grid, resulting in elevated air emissions (CO_2 , NO_x , SO_2).

Furthermore, using pyro-oil to self-supply energy in the process decreases the number of co-products from pyrolysis. Consequently, higher allocation percentages are observed for rejuvenator fractions: 53% for the electric dryer scenario, 70% for the thermal dryer, and 100% for the thermal-ICE scenario. This suggests that in the scenario involving an electric dryer, only 53% of the resources and emissions from waste tire transportation, pre-treatment, pyrolysis, and TPO production contribute to the rejuvenator fraction. On the other hand, higher allocation percentages lead to increased resource consumption and emissions for producing the same quantity of rejuvenator. As a result, the thermal dryer coupled with ICE demonstrates adverse impacts in the aforementioned categories, underscoring the significance of considering the broader environmental implications when assessing alternative drying systems.

The study's findings suggest that while the thermal dryer and thermal dryer-ICE scenarios reduce dependence on the national electricity mix and alleviate fossil resource scarcity, they also entail trade-offs. For instance, both scenarios resulted in increased carbon emissions, leading to higher impacts in certain environmental categories. However, the advantages of the thermal-based drying alternatives were confirmed when the ReCiPe endpoint approach was applied. The results of the comparison revealed that the thermal dryer combined with the ICE energy recuperation strategy has the lowest total environmental impact, with a score of 91.4 millipoints (mPt), outperforming both thermal (106 mPt) and electrical dryers (152 mPt), respectively. This result suggests that exploring alternative encapsulation technologies, or improving existing processes, is a priority to enhance the sustainability and environmental competitiveness of encapsulated pyro-rejuvenators.

Table 4. Environmental impacts of implementing several energy-recuperation strategies. Impacts were analyzed for one kilogram (kg) of capsules as the functional unit (FU).

Impact categories	Unit	Electric dryer	Thermal dryer	Thermal dryer-ICE
Global warming	kg CO ₂ eq	1.495	1.710	3.850
Stratospheric ozone depletion	kg CFC11 eq	3E-07	2.2E-07	2.4E-07
Ozone formation, Human health	kg NO _x eq	0.0047	0.0033	0.0258
Fine particulate matter formation	kg PM _{2.5} eq	0,0118	0.0073	0.0027
Ozone formation, Terrestrial ecosystems	kg NO _x eq	0.0047	0.0034	0.0461
Terrestrial acidification	kg SO ₂ eq	5.5E-06	6.3E-06	32E-06
Freshwater eutrophication	kg P eq	9.6E-05	6.3E-05	2.3E-05
Marine eutrophication	kg N eq	2.3E-06	1.8E-06	1.1E-06
Terrestrial ecotoxicity	kg 1,4-DCB	1.420	1.410	1.520
Freshwater ecotoxicity	kg 1,4-DCB	6.4E-04	4.8E-04	3.1E-04
Marine ecotoxicity	kg 1,4-DCB	0.0016	0.0014	0.0012
Human carcinogenic toxicity	kg 1,4-DCB	0.0037	0.0025	0.0009
Human non-carcinogenic toxicity	kg 1,4-DCB	0.173	0.117	0.052
Land use	m ² a crop eq	0.012	0.0084	0.0041

Mineral resource scarcity	kg _{Cu eq}	8.8E-05	8.6E-05	8.31E-05
Fossil resource scarcity	kg _{oil eq}	0.349	0.222	0.072
Water consumption	m ³	0.018	0.017	0.016
Total impact *	mPt/FU	152	106	91.4

*Using ReCiPe Endpoint H/World (2010) H/A

In addition to energy, water requirements for the encapsulation stages represent the largest contribution (98% in Fig. 9) to the total water consumption category in the process. This is mainly associated with the preparation of low-concentration alginate emulsions and hardening CaCl₂ solutions as well as the washing/filtering of capsules. Specifically, the emulsification process requires 10.3 kg of deionized water per kilogram of capsules, while the washing process needs 4 kg of process water per kilogram of capsules. This water usage could present challenges during the technology's implementation, especially considering plans to locate the plant in mining regions, particularly in northern Chile. Nonetheless, these regions are characterized by a high-water stress index (WSI=1) (Rodríguez-Merchan et al., 2021). Therefore, our findings highlight the need to optimize water usage through strict control strategies and recycling loops. Additionally, exploring alternative water sources, such as desalinated seawater, is crucial to addressing potential challenges related to water scarcity. This technology is already mature and available in northern Chile; however, further experimentation is needed to validate its chemical suitability (e.g., potential interference of salt ions during the gelation or capsule hardening processes). As well, new environmental impacts may arise from desalination, such as harmful algal blooms, the disposal of desalination concentrate, and the high energy consumption associated with water supply systems (Herrera-León et al., 2019).

The comparative analysis between our findings and the existing literature was constrained by the limited availability of similar studies. Only one relevant study was found in this context, conducted by Moins et al., (2022). In their study, Moins et al., (2022) investigated the environmental impacts associated to three distinct road design alternatives (considering no recycling, reclaimed asphalt pavement, and reclaimed asphalt pavement with rejuvenators), encompassing the manufacturing of rejuvenators. This study did not consider the encapsulation of the rejuvenator. Despite they do not included details on the production process

or composition of the used rejuvenators, they provided an estimated environmental impact of producing liquid rejuvenator ranging from 90.80 to 224.61 points per ton, utilizing ReCiPe 2016 hierarchist (H) method. However, it is crucial to emphasize that the analyses of environmental impacts are highly sensitive to factors such as system boundaries, allocation principles, process efficiency, rejuvenator production pathways, as well as the completeness and representativeness of the input data. Additionally, the representativeness of temporal data can significantly impact the results of the LCA. To mitigate this issue, here average or historical inventory data for foreground and background systems were used for attributional life cycle assessment. For foreground systems, the timing of data collection was not considered, which according to Beloin-Saint-Pierre et al., (2020) and Cardellini et al., (2018) may imply limitations and uncertainties for LCA outcomes. Nevertheless, these limitations are reduced here as pyrolysis is a mature technology for tire valorization with low variations of the operation factors over time, thus the presented data inventory is quite representative.

Conversely, we consider that major deviations may occur in the context of encapsulation, as this is a novel and less mature technology, with no existing commercial plants available to validate inventory data. To solve these problems, inventory data was extrapolated from laboratory results utilizing scaling-up approaches based on equipment technical attributes and professional skills, as is a usual practice for new technologies (Spreafico et al., 2024). Another significant problem is the intrinsic temporal changes of Chile's electricity grid, which change during the day, week, month, and season. To account for this unpredictability, the analysis assumed an annual average for 2022. Nonetheless, significant changes happened in 2023, with coal's contribution to the energy mix falling from 23% to 17% and the share of renewable energy sources rising from 54% to 63%. As demonstrated in this study, the electricity matrix significantly impacts environmental outcomes, making it a critical factor in the life cycle of encapsulation and rejuvenation technologies. Therefore, the intrinsic temporal fluctuations in Chile's energy supply must be carefully analyzed in future LCA studies using dynamic LCA methods (Naumann et al., 2024).

4. CONCLUSIONS

The conversion of mining truck waste tires into encapsulated pyro-rejuvenators for asphalt self-healing offers a viable solution from both technical and environmental perspectives. Our investigation reveals that:

- Pyrolysis of mining truck tires at 470 °C can yield up to 54.3 kg of tire pyrolysis oil per kg of tire. After distillation between 160 – 200 °C, this crude oil leads to a pyro-rejuvenator containing monoaromatics BTX (14.6%), *o*-cymene (10.9%), and limonene (57.7%), with a density of 0.832 g/cm³ and viscosity below 10 cP.
- The encapsulation efficiency of the pyro-rejuvenator within alginate-based capsules was 97%, although the process is water and energy-intensive, requiring 14.18 m³ of water and 1.36 MWth per ton of capsules.
- The integrated mass balances of the pyrolysis, distillation, and encapsulation processes yield 270 kg of pyro-rejuvenator, 11 kg of heavy fuel, 10 kg of light fuel, and 5 kg of pyro-gas per ton of waste tires processed.
- Environmental analysis shows that gaseous emissions from TPO and TPG combustion and water use during encapsulation are the main consequences of process impacts. Despite these concerns, our findings match commercial asphalt rejuvenators' impact points per ton of pyro-rejuvenator generated.

This research provides the first analysis of the technical and environmental impacts of encapsulated pyro-rejuvenators derived from mining truck waste tires. The study encourages sustainable practices in chemistry and engineering, supporting the asphalt industry's adoption of rejuvenators to develop more sustainable and resilient self-healing roads.

5. ACKNOWLEDGEMENTS

This research was funded by the National Research and Development Agency (ANID) from the Government of Chile, through the Research Projects FONDEF No. ID21I10127 and ANID/FONDAP/15130015 and ANID/FONDAP/1523A0001.

6. REFERENCES

- Arteaga-Pérez, L.E., Casas-Ledón, Y., Prins, W., Radovic, L., 2014. Thermodynamic predictions of performance of a bagasse integrated gasification combined cycle under quasi-equilibrium conditions. *Chemical Engineering Journal* 258, 402–411. <https://doi.org/10.1016/j.cej.2014.07.104>
- ASTM D86-23, 2024. Standard Test Method for Distillation of Petroleum Products and Liquid Fuels at Atmospheric Pressure [WWW Document]. ASTM. URL <https://www.astm.org/d0086-23ae02.html> (accessed 12.11.24).
- Beloin-Saint-Pierre, D., Albers, A., Hélias, A., Tiruta-Barna, L., Fantke, P., Levasseur, A., Benetto, E., Benoist, A., Collet, P., 2020. Addressing temporal considerations in life cycle assessment. *Science of The Total Environment* 743, 140700. <https://doi.org/10.1016/j.scitotenv.2020.140700>
- Biblioteca del Congreso Nacional, 2016. Biblioteca del Congreso Nacional | Ley Chile [WWW Document]. www.bcn.cl/leychile. URL <https://www.bcn.cl/leychile> (accessed 12.11.24).
- Cámara del Neumático en Chile, 2024. Generación de NFU por regiones en Chile [WWW Document]. Generación de NFU. URL <https://cinc.cl/estadisticas/>
- Campuzano, F., Abdul Jameel, A.G., Zhang, W., Emwas, A.H., Agudelo, A.F., Martínez, J.D., Sarathy, S.M., 2021a. On the distillation of waste tire pyrolysis oil: A structural characterization of the derived fractions. *Fuel* 290. <https://doi.org/10.1016/j.fuel.2020.120041>
- Campuzano, F., Abdul Jameel, A.G., Zhang, W., Emwas, A.H., Agudelo, A.F., Martínez, J.D., Sarathy, S.M., 2021b. On the distillation of waste tire pyrolysis oil: A structural characterization of the derived fractions. *Fuel* 290. <https://doi.org/10.1016/j.fuel.2020.120041>
- Campuzano, F., Abdul Jameel, A.G., Zhang, W., Emwas, A.-H., Agudelo, A.F., Martínez, J.D., Sarathy, S.M., 2020. Fuel and Chemical Properties of Waste Tire Pyrolysis Oil Derived from a Continuous Twin-Auger Reactor. *Energy & Fuels* 34, 12688–12702. <https://doi.org/10.1021/acs.energyfuels.0c02271>
- Campuzano, F., Martínez, J.D., Agudelo Santamaría, A.F., Sarathy, S.M., Roberts, W.L., 2023. Pursuing the End-of-Life Tire Circularity: An Outlook toward the Production of Secondary Raw Materials

- from Tire Pyrolysis Oil. *Energy Fuels* 37, 8836–8866.
<https://doi.org/10.1021/acs.energyfuels.3c00847>
- Cardellini, G., Mutel, C.L., Vial, E., Muys, B., 2018. Temporalis, a generic method and tool for dynamic Life Cycle Assessment. *Science of The Total Environment* 645, 585–595.
<https://doi.org/10.1016/j.scitotenv.2018.07.044>
- Cartes, J., Neumann, P., Hospido, A., Vidal, G., 2018. Life cycle assessment of management alternatives for sludge from sewage treatment plants in Chile: does advanced anaerobic digestion improve environmental performance compared to current practices? *J Mater Cycles Waste Manag* 20, 1530–1540. <https://doi.org/10.1007/s10163-018-0714-9>
- Chávez-Delgado, M., Colina, J.R., Segura, C., Álvarez, C., Osorio-Vargas, P., Arteaga-Pérez, L.E., Norambuena-Contreras, J., 2024. Asphalt pyro-rejuvenators based on waste tyres: An approach to improve the rheological and self-healing properties of aged binders. *Journal of Cleaner Production* 452. <https://doi.org/10.1016/j.jclepro.2024.142179>
- Comisión Nacional de Energía, 2022. Generación Bruta ERNC – Energía Abierta [WWW Document]. Generación Bruta ERNC – Energía Abierta | Comisión Nacional de Energía. URL <http://energiaabierta.cl/visualizaciones/generacion-bruta-ernc/> (accessed 12.11.24).
- Concha, J.L., Arteaga-Pérez, L., Gonzalez-Torre, I., Norambuena-Contreras, J., 2021. Biocapsules containing low-cost rejuvenators for asphalt self-healing. *RILEM Tech Lett* 6, 1–7.
<https://doi.org/10.21809/rilemtechlett.2021.129>
- Concha, J.L., Delgadillo, R., Arteaga-Pérez, L.E., Segura, C., Norambuena-Contreras, J., 2023. Optimised Sunflower Oil Content for Encapsulation by Vibrating Technology as a Rejuvenating Solution for Asphalt Self-Healing. *Polymers*. <https://doi.org/10.3390/polym15061578>
- Concha, J.L., Viana-Sepulveda, A., Caro, S., Arteaga-Pérez, L.E., Norambuena-Contreras, J., 2024. Dynamic mechanical analysis of asphalt mortar samples containing millimetre-size capsules for self-healing purposes. *Powder Technology* 440, 119735.
<https://doi.org/10.1016/j.powtec.2024.119735>

- Dewulf, J., Van Langenhove, H., 2005. Integrating industrial ecology principles into a set of environmental sustainability indicators for technology assessment. *Resources, Conservation and Recycling* 43, 419–432. <https://doi.org/10.1016/j.resconrec.2004.09.006>
- Energía Abierta, 2023. Balance Nacional de Energía [WWW Document]. Energía Abierta. URL <http://energiaabierta.cl/visualizaciones/balance-de-energia/> (accessed 12.1.24).
- François, J., Mauviel, G., Feidt, M., Rogaume, C., Rogaume, Y., Mirgaux, O., Patisson, F., Dufour, A., 2013. Modeling of a Biomass Gasification CHP Plant: Influence of Various Parameters on Energetic and Exergetic Efficiencies. *Energy Fuels* 27, 7398–7412. <https://doi.org/10.1021/ef4011466>
- Gonzalez-Torre, I., Norambuena-Contreras, J., 2020. Recent advances on self-healing of bituminous materials by the action of encapsulated rejuvenators. *Construction and Building Materials* 258, 119568. <https://doi.org/10.1016/j.conbuildmat.2020.119568>
- Herrera-León, S., Cruz, C., Kraslawski, A., Cisternas, L.A., 2019. Current situation and major challenges of desalination in Chile. *Desalination and Water Treatment* 171, 93–104. <https://doi.org/10.5004/dwt.2019.24863>
- ISO, 2006. ISO 14044:2006(es), Gestión ambiental — Análisis del ciclo de vida — Requisitos y directrices [WWW Document]. URL <https://www.iso.org/obp/ui/#iso:std:iso:14044:ed-1:v1:es> (accessed 12.11.24).
- Jungbluth, N., Frischknecht, R., 2006. Life Cycle Inventory Analysis Applied to Renewable Resources, in: *Renewables-Based Technology*. John Wiley & Sons, Ltd, pp. 55–72. <https://doi.org/10.1002/0470022442.ch4>
- Khan, K., Ahmad, W., Amin, M.N., Khan, S.A., Deifalla, A.F., Younes, M.Y.M., 2023. Research evolution on self-healing asphalt: A scientometric review for knowledge mapping. *REVIEWS ON ADVANCED MATERIALS SCIENCE* 62. <https://doi.org/10.1515/rams-2022-0331>
- Kumar, Ankush, Choudhary, R., Kumar, Abhinay, 2022. Evaluation of Waste Tire Pyrolytic Oil as a Rejuvenation Agent for Unmodified, Polymer-Modified, and Rubber-Modified Aged Asphalt

- Binders. *Journal of Materials in Civil Engineering* 34, 04022246.
[https://doi.org/10.1061/\(ASCE\)MT.1943-5533.0004400](https://doi.org/10.1061/(ASCE)MT.1943-5533.0004400)
- Kyklos, 2021. Estudio del Material Disponible País y el reciclado de los productos prioritarios en Chile, 2021 [WWW Document]. URL https://www.anir.cl/wp-content/uploads/2022/12/ANIR2021-NFU-Estudio_del_material_disponible_País.pdf
- Larrere, S., 2023. Análisis de ciclo de vida del proceso de encapsulamiento de rejuvenecedores pirolíticos para su uso en mezclas asfálticas autorreparables (Ingeniería Química). Universidad del Bío-Bío, Chile.
- Li, C., Rajib, A., Sarker, M., Liu, R., Fini, E.H., Cai, J., 2021. Balancing the Aromatic and Ketone Content of Bio-oils as Rejuvenators to Enhance Their Efficacy in Restoring Properties of Aged Bitumen. *ACS Sustainable Chem. Eng.* 9, 6912–6922. <https://doi.org/10.1021/acssuschemeng.0c09131>
- Li, Y., Hao, P., Zhang, M., 2021. Fabrication, characterization and assessment of the capsules containing rejuvenator for improving the self-healing performance of asphalt materials: A review. *Journal of Cleaner Production* 287, 125079. <https://doi.org/10.1016/j.jclepro.2020.125079>
- M. Díaz, 2024. Declaración de impacto Ambiental: Planta de valorización de neumáticos fuera de uso [WWW Document]. Sistema de Declaración de Impactos Ambientales. URL https://seia.sea.gob.cl/expediente/ficha/fichaPrincipal.php?modo=normal&id_expediente=2153557673 (accessed 12.11.24).
- Magdalena; Cardemil-Winkler, 2020. Impactos socioeconómicos de la minería en Chile. - Asesorías Parlamentarias BCN. Búsqueda por Categoría Temática [WWW Document]. bcn.cl. URL <https://www.bcn.cl/asesoriasparlamentarias/www.bcn.clid=81438> (accessed 12.11.24).
- Martínez, J.D., Campuzano, F., Agudelo, A.F., Cardona-Uribe, N., Arenas, C.N., 2021. Chemical recycling of end-of-life tires by intermediate pyrolysis using a twin-auger reactor: Validation in a laboratory environment. *Journal of Analytical and Applied Pyrolysis* 159, 105298. <https://doi.org/10.1016/j.jaap.2021.105298>

- Martínez, J.D., Cardona-Urbe, N., Murillo, R., García, T., López, J.M., 2019. Carbon black recovery from waste tire pyrolysis by demineralization: Production and application in rubber compounding. *Waste Management* 85, 574–584.
- Martínez, J.D., Puy, N., Murillo, R., García, T., Navarro, M.V., Mastral, A.M., 2013. Waste tyre pyrolysis - A review. *Renewable and Sustainable Energy Reviews* 23, 179–213. <https://doi.org/10.1016/j.rser.2013.02.038>
- Menares, T., Herrera, J., Romero, R., Osorio, P., Arteaga-Pérez, L.E., 2020. Waste tires pyrolysis kinetics and reaction mechanisms explained by TGA and Py-GC/MS under kinetically-controlled regime. *Waste Management* 102, 21–29. <https://doi.org/10.1016/j.wasman.2019.10.027>
- Moins, B., Hernando, D., Buyle, M., France, C., Van den bergh, W., Audenaert, A., 2022. On the road again! An economic and environmental break-even and hotspot analysis of reclaimed asphalt pavement and rejuvenators. *Resources, Conservation and Recycling* 177, 106014. <https://doi.org/10.1016/j.resconrec.2021.106014>
- Naumann, G., Famiglietti, J., Schropp, E., Motta, M., Gaderer, M., 2024. Dynamic life cycle assessment of European electricity generation based on a retrospective approach. *Energy Conversion and Management* 311, 118520. <https://doi.org/10.1016/j.enconman.2024.118520>
- Norambuena-Contreras, J., Arteaga-Pérez, L.E., Concha, J.L., Gonzalez-Torre, I., 2021. Pyrolytic oil from waste tyres as a promising encapsulated rejuvenator for the extrinsic self-healing of bituminous materials. *Road Materials and Pavement Design* 22, S117–S133. <https://doi.org/10.1080/14680629.2021.1907216>
- Norambuena-Contreras, J., Concha, J.L., Arteaga-Pérez, L.E., Gonzalez-Torre, I., 2022. Synthesis and Characterisation of Alginate-Based Capsules Containing Waste Cooking Oil for Asphalt Self-Healing. *Applied Sciences* 12, 2739. <https://doi.org/10.3390/app12052739>
- Osorio-Vargas, P., Lick, I.D., Sobrevía, F., Correa-Muriel, D., Menares, T., Manrique, R., Casella, M.L., Arteaga-Pérez, L.E., 2021. Thermal Behavior, Reaction Pathways and Kinetic Implications of

- Using a Ni/SiO₂ Catalyst for Waste Tire Pyrolysis. Waste and Biomass Valorization. <https://doi.org/10.1007/s12649-021-01494-y>
- Pourhashem, G., Spatari, S., Boateng, A.A., McAloon, A.J., Mullen, C.A., 2013. Life Cycle Environmental and Economic Tradeoffs of Using Fast Pyrolysis Products for Power Generation. *Energy Fuels* 27, 2578–2587. <https://doi.org/10.1021/ef3016206>
- Quezada, G.R., Solar, C., Saavedra, J.H., Petit, K., Martin-Martínez, F.J., Arteaga-Pérez, L.E., Norambuena-Contreras, J., 2024. Operando FTIR-ATR with molecular dynamic simulations to understand the diffusion mechanism of waste tire-derived pyrolytic oil for asphalt self-healing. *Fuel* 357, 129834. <https://doi.org/10.1016/j.fuel.2023.129834>
- Ren, S., Liu, X., Lin, P., Gao, Y., Erkens, S., 2022. Review on the diffusive and interfacial performance of bituminous materials: From a perspective of molecular dynamics simulation. *Journal of Molecular Liquids* 366, 120363. <https://doi.org/10.1016/j.molliq.2022.120363>
- Rodríguez-Merchan, V., Ulloa-Tesser, C., Baeza, C., Casas-Ledón, Y., 2021. Evaluation of the Water–Energy nexus in the treatment of urban drinking water in Chile through exergy and environmental indicators. *Journal of Cleaner Production* 317, 128494. <https://doi.org/10.1016/j.jclepro.2021.128494>
- Rodríguez-Machín, L., Ronsse, F., Casas-Ledón, Y., Arteaga-Pérez, L.E., 2021. Fast pyrolysis of raw and acid-leached sugarcane residues *en route* to producing chemicals and fuels: Economic and environmental assessments. *Journal of Cleaner Production* 296, 126601. <https://doi.org/10.1016/j.jclepro.2021.126601>
- Sinnott, R., Towler, G., 2013. *Chemical Engineering Design - Principles, Practice and Economics of Plant and Process Design Second Edition*, Chemical Engineering Design. <https://doi.org/10.1016/B978-0-08-096659-5.00022-5>
- Spreafico, C., Thonemann, N., Pizzol, M., Arvidsson, R., Steubing, B., Cucurachi, S., Cardellini, G., Spreafico, M., 2024. Using patents to support prospective life cycle assessment: opportunities and limitations. *Int J Life Cycle Assess.* <https://doi.org/10.1007/s11367-024-02404-9>

Wan, P., Wu, S., Liu, Q., Zou, Y., Zhao, Z., Chen, S., 2022. Recent advances in calcium alginate hydrogels encapsulating rejuvenator for asphalt self-healing. *Journal of Road Engineering* 2, 181–220.

<https://doi.org/10.1016/j.jreng.2022.06.002>

Wu, Q., Zhang, Q., Chen, X., Song, G., Xiao, J., 2022. Integrated Assessment of Waste Tire Pyrolysis and Upgrading Pathways for Production of High-Value Products. *ACS Omega* 7, 30954–30966.

<https://doi.org/10.1021/acsomega.2c02952>

Journal Pre-proof

Highlights

- A model for waste tires pyrolysis integrated with TPO upgrading and encapsulation.
- Aromatic and terpenic content of distilled TPO supports its rejuvenation capacity.
- Waste tire pyrolytic oil was efficiently encapsulated into biopolymeric matrices.
- Encapsulation caused the major environmental impacts due to water and e-consumption.

Journal Pre-proof

Declaration of interests

The authors declare that they have no known competing financial interests or personal relationships that could have appeared to influence the work reported in this paper.

The authors declare the following financial interests/personal relationships which may be considered as potential competing interests:

Journal Pre-proof